

Polarization in cyclotron radiation in strong magnetic fields

Luidmila Semionova¹, Denis Leahy² and Jorge Paez³

¹ Department of Physics, Universidad Nacional, Heredia 86–3000, Costa Rica;
lsemiono@yahoo.com

² Department of Physics and Astronomy, University of Calgary, Alberta T2N 1N4, Canada;
leahy@iras.ucalgay.ca

³ Space Research Center, University of Costa Rica, San Jose, Costa Rica;
paezjorge174@gmail.com

Received 2009 July 14; accepted 2010 March 23

Abstract We revisit the problem of radiative transitions of electrons in the presence of a strong magnetic field. We derive fully relativistic cyclotron transition rates for an arbitrary magnetic field, for any orientation of electron spin and for any polarization of the emitted radiation. Also, we obtain the transition rates for any value of the initial electron's parallel momentum. For very strong magnetic fields, transitions to the ground state predominate. Transition rates summed over the electron's spin orientation and for unpolarized radiation are also obtained, which confirm previous results by Latal. Transition widths are calculated for different electron spin orientations and different polarizations of radiation. We obtain general expressions for transition rates that reduce to the results for the non-relativistic case and for unpolarized radiation. Additionally we get, for the non-relativistic approximation, the transition rates for any polarization of radiation. As an application, the first five emission lines are evaluated and compared to the X-ray emitting neutron star V0332+53, which has multiple observable cyclotron lines, taking into account gravitational redshift. The most probable polarization is $\hat{\epsilon}^{(2)}$.

Key words: stars: neutron — radiation mechanisms: non-thermal — stars: magnetic fields — polarization

1 INTRODUCTION

Cyclotron transition rates in strong magnetic fields are of great interest for emission from neutron stars and some other exotic magnetized stellar objects, and have been discussed many times previously. Particularly, the effect of initial electron's spin orientation on cyclotron radiation has been analyzed by Herold et al. (1982). In that work, the transition rates are summed over the final spin state and polarization of the emitted radiation. Harding & Preece (1987) discussed the behavior of cyclotron transition rates as a function of electron spin for both initial and final states, unpolarized radiation, and the case of zero initial electron parallel momentum. Bezchastnov & Pavlov (1991) discuss cyclotron emission in plasmas including quantum and relativistic effects, but summed over electron spin. A study of the effects of polarization of the emitted photon can be found in Sina (1996), in which the angular distribution of radiation for two linear polarizations was analyzed, but

considering only zero initial parallel electron momentum. Latal (1986) considered the radiative transition of the electron between low-lying Landau levels and the ground state in high magnetic fields. He obtained transitions rates without taking into account the polarization of radiation, but for different orientations of the electron's spin in the initial state. We extend this evaluation further, including the different possible polarization of photons. Also we obtain the transition rates for any N value of the final state, and for any orientation of the electron's spin if N is different from zero. Pavlov et al. (1991) studied cyclotron radiation in strong magnetic fields but did not take into account the consideration of polarizations of the photons. Baring et al. (2005) developed previous results in the literature to obtain compact analytical expressions for cyclotron decay rates and widths in terms of a series of Legendre functions of the second kind. Thus, they explicitly obtain the transition rates for any third component of momentum of an electron, but only for transitions to the fundamental state and without taking into account the polarization of radiation and the polarization of the electron's spin orientation if the final state is different from zero. Here, we generalize the previous studies, including arbitrary electron Landau levels and spin states, electron parallel momentum and radiation polarization states, and derive new expressions for the transition rates.

2 THE S-MATRIX

Cyclotron emission is a first order process, and the Feynman graph is shown, e.g., in Daugherty & Ventura (1978). Here we use natural units, in which $c = \hbar = 1$, so, e.g., $B_{\text{cr}} = \frac{m^2}{e} = 4.414 \times 10^{13}$ G. In a magnetic field, the electron Landau energy level is given by $E_N = [p_z^2 + m^2 + 2NeB]^{1/2}$, or by $E_N = [p_z^2 + m^2(1 + 2NB')]^{1/2}$, with $B' = \frac{B}{B_{\text{cr}}}$. We keep non-zero p_z in our expressions, although it has been pointed out several times previously that one can carry out calculations for $p_z=0$, then perform a Lorentz transformation into a frame with non-zero p_z . When we present figures showing computed results, we present just $p_z=0$ cases for simplicity. The reason for keeping non-zero p_z in our formulae, even though they are more complex, is to allow calculations to be made for non-zero p_z , since in some cases it may be simpler to carry out these calculations. Examples could be a complex velocity distribution where calculating the results which are directly dependent on p_z might be simpler than carrying out the set of Lorentz transformations (one for each velocity), or if one was calculating a quantity which is not Lorentz-covariant, in which case one could not use the Lorentz transformation. The S-matrix element for cyclotron emission is

$$S_{fi} = (-ie) \int_{-\infty}^{\infty} dt \int_{-\infty}^{\infty} d^3x \bar{\Psi}_f(x) A^\mu(x) \Psi_i(x), \quad (1)$$

where $\Psi_f(x)$ is the wave function of the electron (see Appendix) and $A^\mu(x)$ is the photon emission wave function

$$A^\mu(x) = \frac{\varepsilon^\mu}{[2\omega V]^{1/2}} e^{ik_\nu x^\nu} = \frac{\varepsilon^\mu}{[2\omega V]^{1/2}} e^{i\omega t - i\mathbf{k}\mathbf{x}}, \quad (2)$$

where the polarization of the photon $\hat{\varepsilon}^\mu$ can be denoted by $\lambda = 1, 2$ (linear polarization) or $\lambda = +, -$ (right and left handed circular polarization), i.e., $\hat{\varepsilon}^{(1)}$ also represents parallel polarization and $\hat{\varepsilon}^{(2)}$ represents perpendicular polarization, where the photon's electric field is parallel or perpendicular to $\mathbf{k} \times \mathbf{B}$, respectively. $\hat{\varepsilon}^{(3)}$ means the third component of the polarization of the photon along the magnetic field B . V means the underlying periodicity volume. Explicitly, the linear polarization unit vectors are given by

$$\hat{\varepsilon}^{(1)} = -\cos\theta \cos\varphi \hat{i} - \cos\theta \sin\varphi \hat{j} + \sin\theta \hat{k}, \quad (3)$$

$$\hat{\varepsilon}^{(2)} = \sin\varphi \hat{i} - \cos\varphi \hat{j}, \quad (4)$$

where θ, φ are spherical polar coordinates of the photon. The two circular polarizations are given by

$$\hat{\varepsilon}_\pm = \mp \frac{1}{\sqrt{2}} [\hat{\varepsilon}^{(1)} \pm i\hat{\varepsilon}^{(2)}]. \quad (5)$$

Thus, the photon momentum vector is

$$\mathbf{k} = \omega[\sin \theta \cos \varphi \hat{i} + \sin \theta \sin \varphi \hat{j} + \cos \theta \hat{k}]. \quad (6)$$

The S -matrix element for the cyclotron radiation process for the cases of non-spin flip transitions (initial and final electron spins down-down $\downarrow\downarrow$, or initial and final electron spins up-up $\uparrow\uparrow$) is

$$\begin{aligned} S_{fi}^{r,r'} = & \frac{-ie[eB]^{1/2}}{4L_z L_y [EE_0(E+E_0)]^{1/2} [E'E'_0(E'+E'_0)]^{1/2}} \frac{[2\pi]^3}{[2\omega V]^{1/2}} \\ & \delta(E' - E - \omega) \delta(p'_y - p_y - k_y) \delta(p'_z - p_z - k_z) \\ & \cdot [i\varepsilon_-(E_0 + rm)(E'_0 - r'm)^{1/2} \cdot [(E + E_0)(E' + E'_0) - p_z p'_z] \cdot I_1 \\ & + \varepsilon^{3(\lambda)}(E_0 + rm)^{1/2}(E'_0 + r'm)^{1/2} \cdot [p_z(E' + E'_0) + p'_z(E + E_0)] \cdot I_2 \\ & + i\varepsilon_+(E_0 - rm)(E'_0 + r'm)^{1/2} [p_z p'_z - (E + E_0)(E' + E'_0)] \cdot I_3 \\ & + \varepsilon^{3(\lambda)}(E_0 - rm)^{1/2}(E'_0 - r'm)^{1/2} \cdot [p_z(E' + E'_0) + p'_z(E + E_0)] \cdot I_4], \quad (7) \end{aligned}$$

where the superscripts on S denote initial and final spin states ($r = r' = 1$ for the case of $\uparrow\uparrow$ and $r = r' = -1$ for the case of $\downarrow\downarrow$).

For the spin-flip transitions $r \neq r'$, i.e. $\uparrow\downarrow$ and $\downarrow\uparrow$, the S -matrix element is given by

$$\begin{aligned} S_{fi}^{r,r'} = & \frac{[-ie][eB]^{1/2}}{4L_z L_y [EE_0(E+E_0)]^{1/2} [E'E'_0(E'+E'_0)]^{1/2}} \frac{[2\pi]^3}{[2\omega V]^{1/2}} \\ & \delta(E' - E - \omega) \delta(p'_y - p_y - k_y) \delta(p'_z - p_z - k_z) \\ & \cdot [r'\varepsilon_-(E_0 + rm)(E'_0 - r'm)^{1/2} [p'_z(E + E_0) - p_z(E' + E'_0)] \cdot I_1 \\ & + ir'\varepsilon^{3(\lambda)}(E_0 + rm)^{1/2}(E'_0 + r'm)^{1/2} [p_z p'_z + (E + E_0)(E' + E'_0)] \cdot I_2 \\ & + r'\varepsilon_+(E_0 - rm)(E'_0 + r'm)^{1/2} [p'_z(E + E_0) - p_z(E' + E'_0)] \cdot I_3 \\ & - ir'\varepsilon^{3(\lambda)}(E_0 - rm)^{1/2}(E'_0 - r'm)^{1/2} [p_z p'_z + (E + E_0)(E' + E'_0)] \cdot I_4]. \quad (8) \end{aligned}$$

3 TRANSITION RATES

The differential transition rates for the four cases can be written as just one expression as follows:

$$\begin{aligned} dW_{N' \rightarrow N}^{r',r} = & \frac{\alpha \omega d\Omega}{16(2\pi)[E_0(E+E_0)][E'E'_0(E'+E'_0)][E' - \omega(\sin \theta)^2 - p'_z \cos \theta]} \cdot \\ & \left[\left(\frac{[p'_z(E + E_0) - p_z(E' + E'_0)]_{r \neq r'}^2}{[(E + E_0)(E' + E'_0) - p_z p'_z]_{r=r'}^2} \right) \right. \\ & [\varepsilon_- \varepsilon_-^*(E_0 + rm)(E'_0 - r'm) I_{N',N-1}^2(x) + \varepsilon_+ \varepsilon_+^*(E_0 - rm)(E'_0 + r'm) I_{N'-1,N}^2(x)] \\ & + \sqrt{2N'eB} [(E + E_0)(E' + E'_0) - rr'p_z p'_z] [p_z(E' + E'_0) + rr'p'_z(E + E_0)] \\ & [(E_0 + rm)(\varepsilon_- \varepsilon_-^{*3(\lambda)} e^{i\varphi} + \varepsilon_-^{3(\lambda)} \varepsilon_-^* e^{-i\varphi}) I_{N',N-1}(x) I_{N'-1,N-1}(x) \\ & + (E_0 - rm)(\varepsilon_+ \varepsilon_+^{*3(\lambda)} e^{-i\varphi} + \varepsilon_+^{3(\lambda)} \varepsilon_+^* e^{i\varphi}) I_{N'-1,N}(x) I_{N',N}(x)] \\ & + 2rr'eB\sqrt{NN'} \left[\left(\frac{[p'_z(E + E_0) - p_z(E' + E'_0)]_{r \neq r'}^2}{[(E + E_0)(E' + E'_0) - p_z p'_z]_{r=r'}^2} \right) \right. \\ & (\varepsilon_- \varepsilon_+^* e^{i2\cdot\varphi} + \varepsilon_+ \varepsilon_-^* e^{-i2\cdot\varphi}) I_{N',N-1}(x) I_{N'-1,N}(x) \\ & \left. + 2[\varepsilon^{3(\lambda)} \varepsilon^{*3(\lambda)} \left(\frac{[p_z p'_z + (E + E_0)(E' + E'_0)]_{r \neq r'}^2}{[p'_z(E + E_0) + p_z(E' + E'_0)]_{r=r'}^2} \right) I_{N'-1,N-1}(x) I_{N',N}(x) \right] \end{aligned}$$

$$\begin{aligned}
& +\sqrt{2eBN}[(E + E_0)(E' + E'_0) - rr'p_z p'_z][p'_z(E + E_0) + rr'p_z(E' + E'_0)] \\
& [(E'_0 - r'm)(\varepsilon_- \varepsilon^{*3(\lambda)} e^{i\cdot\varphi} + \varepsilon^{3(\lambda)} \varepsilon_-^* e^{(-i\varphi)}) I_{N',N-1}(x) I_{N',N}(x) \\
& + (E'_0 + r'm)[\varepsilon_+ \varepsilon^{*3(\lambda)} e^{-i\cdot\varphi} + \varepsilon^{3(\lambda)} \varepsilon_+^* e^{i\cdot\varphi}] I_{N'-1,N-1}(x) I_{N'-1,N}(x)] \\
& + \varepsilon^{3(\lambda)} \varepsilon^* \varepsilon^{3(\lambda)} \cdot \left(\frac{[p_z p'_z + (E + E_0)(E' + E'_0)]_{r \neq r'}^2}{[p'_z(E_0 + E) + p_z(E' + E'_0)]_{r=r'}^2} \right) \\
& \cdot [(E_0 + rm)(E'_0 + r'm) I_{N'-1,N-1}^2(x) + (E_0 - rm)(E'_0 - r'm) I_{N',N}^2(x)], \quad (9)
\end{aligned}$$

where $x = \frac{\omega^2 \sin^2 \theta}{2eB}$, $\varepsilon_+ = \varepsilon_1^{(\lambda)} + i\varepsilon_2^{(\lambda)}$, $\varepsilon_- = \varepsilon_1^{(\lambda)} - i\varepsilon_2^{(\lambda)}$, and $I_{N',N}(x)$ is the Laguerre function, for which we use the expression

$$I_{N',N} = \frac{\sqrt{N!}}{\sqrt{N'!}} e^{-\frac{\omega^2 \sin^2 \theta}{4eB}} \left(\frac{\omega^2 \sin^2 \theta}{2eB} \right)^{(N'-N)/2} L_N^{N'-N} \left(\frac{\omega^2 \sin^2 \theta}{2eB} \right). \quad (10)$$

The integrals in the S -matrix element I_1 , I_2 , I_3 and I_4 are summarized in the Appendix.

In Table 1 we give the coefficients related to the polarization of the radiation which appear in Equation (9). If we take $p'_z = 0$, and sum over the outgoing electron spin, we obtain a transition rate which is in agreement with Herold et al. (1982).

Table 1 Coefficients Related to Polarization

Coefficient	$\varepsilon^{(\lambda=1)}$	$\varepsilon^{(\lambda=2)}$	$\varepsilon^{(\lambda=\pm)}$	Sum over λ
$\varepsilon_- \varepsilon_-^*$	$(\cos \theta)^2$	1	$\frac{1}{2}(1 \pm \cos \theta)^2$	$1 + (\cos \theta)^2$
$\varepsilon_- \varepsilon^{*3(\lambda)}$	$-\frac{1}{2} \sin 2\theta \cdot e^{-i\cdot\varphi}$	0	$\mp \frac{1}{2} \sin \theta (1 \pm \cos \theta) \cdot e^{-i\cdot\varphi}$	$-\frac{1}{2} \sin 2\theta \cdot e^{-i\cdot\varphi}$
$\varepsilon_- \varepsilon_+^*$	$(\cos \theta)^2 \cdot e^{-i2\cdot\varphi}$	$-e^{-i2\cdot\varphi}$	$-\frac{1}{2} (\sin \theta)^2 \cdot e^{-i2\cdot\varphi}$	$-(\sin \theta)^2 \cdot e^{-i2\cdot\varphi}$
$\varepsilon^{3(\lambda)} \varepsilon_+^*$	$-\frac{1}{2} \sin 2\theta \cdot e^{-i\cdot\varphi}$	0	$\pm \frac{1}{2} \sin \theta (1 \mp \cos \theta) \cdot e^{-i\cdot\varphi}$	$-\frac{1}{2} \sin 2\theta \cdot e^{-i\cdot\varphi}$
$\varepsilon_+ \varepsilon_+^*$	$(\cos \theta)^2$	1	$\frac{1}{2}(1 \mp \cos \theta)^2$	$(1 + [\cos \theta]^2)$
$\varepsilon^{3(\lambda)} \varepsilon^* \varepsilon^{3(\lambda)}$	$(\sin \theta)^2$	0	$\frac{1}{2} (\sin \theta)^2$	$(\sin \theta)^2$

As a consequence of conservation of energy and the parallel component of electron momentum, one has $E' = E + w$ and $p'_z = p_z + w \cdot \cos \theta$.

The energy of the photon as a function of the angle θ is given by

$$\omega_{N' \rightarrow N} = \frac{(E' - p'_z \cos \theta) - \sqrt{(E' - p'_z \cos \theta)^2 - 2m^2 B' \sin^2 \theta (N' - N)}}{\sin^2 \theta}, \quad (11)$$

In Table 2 we give the contributions to the transition rates for different types of polarizations of radiation and use the electron's spin orientation (down-down) in this evaluation. We integrate over the angle θ and take magnetic field values between 5×10^{10} and 4.414×10^{14} G. An important fact is that the most probable polarization of the radiation is $\varepsilon^{(2)}$ rather than $\varepsilon^{(1)}$. Only for a very strong magnetic field, $\sim 4.414 \times 10^{14}$ G, does the transition to the fundamental state dominate, and for $B < 4.414 \times 10^{14}$ G, transitions to the nearest lower level ($N = N' - 1$) dominate. Also seen from Table 2, for $B = 5 \times 10^{12}$ G and $p'_z = 0$, the de-excitation summed over photon polarization is strongly favored via a single step transition. This is consistent with the results of Daugherty & Ventura (1977), in which the photon emission at the specific angle of $\theta = 90^\circ$ was analyzed.

For $p'_z = 0$, the energy of radiation, ω , as a function of θ is

$$\omega_{N' \rightarrow N} = \frac{E'_0 - \sqrt{E'_0{}^2 - 2m^2 B' \sin^2 \theta (N' - N)}}{\sin^2 \theta}. \quad (12)$$

Table 2 Contribution to Transition Rates for Different Types of Polarizations ($p'_z = 0$)

B -magnetic field (G)	$N' \rightarrow N$	$\sum_{\lambda}(\%)$	$\varepsilon^{(\lambda=1)}(\%)$	$\varepsilon^{(\lambda=2)}(\%)$
5×10^{10}	$N' = 2 \rightarrow N = 0$	0.271	0.0451	0.225
	$N' = 2 \rightarrow N = 1$	99.7	25	74.8
	$N' = 3 \rightarrow N = 0$	0.00176	0.00022	0.00154
	$N' = 3 \rightarrow N = 1$	0.538	0.0898	0.448
	$N' = 3 \rightarrow N = 2$	99.5	24.9	74.6
5×10^{12}	$N' = 2 \rightarrow N = 0$	18.3	3.2	15.1
	$N' = 2 \rightarrow N = 1$	81.7	21.7	60
	$N' = 3 \rightarrow N = 0$	6.5	0.875	5.6
	$N' = 3 \rightarrow N = 1$	23.8	4.5	19.3
	$N' = 3 \rightarrow N = 2$	69.7	19.2	50.5
4.414×10^{13}	$N' = 2 \rightarrow N = 0$	45.9	9.6	36.3
	$N' = 2 \rightarrow N = 1$	54.1	16.6	37.5
	$N' = 3 \rightarrow N = 0$	30.7	5.5	25.2
	$N' = 3 \rightarrow N = 1$	28.6	7.2	21.4
	$N' = 3 \rightarrow N = 2$	40.6	12.9	27.8
4.414×10^{14}	$N' = 2 \rightarrow N = 0$	56.3	16.7	39.6
	$N' = 2 \rightarrow N = 1$	43.7	14.5	29.2
	$N' = 3 \rightarrow N = 0$	42	11.8	30.2
	$N' = 3 \rightarrow N = 1$	24.4	7.2	17.2
	$N' = 3 \rightarrow N = 2$	33.6	11.2	22.3

which agrees with equation (15) of Herold et al. (1982). For $\theta = 0^\circ$ or $\theta = 180^\circ$, the photon energy is given by

$$\omega_{N' \rightarrow N} = \frac{(eB)(N - N')}{\pm(p'_z \mp E')}, \quad (13)$$

where the upper sign is for $\theta = 0^\circ$ and the lower sign is for $\theta = 180^\circ$.

For a particular transition from any excited state to the fundamental state $N = 0$, with $p'_z = 0$ and $\theta = 90^\circ$ where ω is maximum, we can write the expression for the emitted energy

$$\begin{aligned} \omega &= m(\sqrt{1 + 2B'N'} - 1) \cdot (1 + Z_g)^{-1} \quad \text{for any } B' \text{ and } N' \\ &\sim mB'N'(1 + Z_g)^{-1} \text{ if } B'N' \ll 1 \text{ or } \omega \sim 11.6 \frac{B}{10^{12} \text{ G}} N'(1 + Z_g)^{-1} \text{ keV,} \end{aligned} \quad (14)$$

(see, Coburn et al. 2002). For the evaluation of the magnetic field strength, we also take into account gravitational redshift

$$Z_g = \left[1 - \frac{R_s}{R}\right]^{-1/2} - 1 \quad (15)$$

with $R_s = \frac{2GM_{\text{NS}}}{c^2}$ and M_{NS} is the mass of the neutron star.

The exact expression for ω (Eq. (14)) must be used when $B' \sim 1$ because otherwise we obtain a significant difference with respect to the exact values, i.e., for $N' = 1 \rightarrow 0$ we get a discrepancy of 38%; for $N' = 2 \rightarrow 0$, 60%; and for $N' = 3 \rightarrow 0$, 80%.

After the integration over ϕ in the equation for the differential transition rate, we obtain the result for any polarization

$$\begin{aligned} \Gamma_{\mp, p'_z=0} &= \frac{\alpha}{2} \int_0^{\frac{\pi}{2}} \frac{d\theta \omega \sin \theta}{E'_0 [E'_0{}^2 - 2eB[N' - N](\sin \theta)^2]^{1/2}} [\varepsilon_- \varepsilon_-^* (E'_0 \pm m)(E'_0 - \omega \mp m) I_{N', N-1}(x)]^2 \\ &\quad - \sqrt{2N'eB\omega} \cos(\theta) [\varepsilon_- \varepsilon_-^{*3(\lambda)} e^{i\varphi} + \varepsilon_-^{3(\lambda)} \varepsilon_-^* e^{-i\varphi}] I_{N', N-1}(x) I_{N'-1, N-1}(x) \\ &\quad + 2eB\sqrt{NN'} I_{N', N-1}(x) I_{N'-1, N}(x) [\varepsilon_- \varepsilon_+^* e^{+i2\varphi} + \varepsilon_+ \varepsilon_-^* e^{-i2\varphi}] \end{aligned}$$

$$\begin{aligned}
& +\varepsilon^{3(\lambda)}\varepsilon^{*3(\lambda)}(E'_0 \mp m)(E'_0 - \omega \pm m)I_{N'-1, N-1}(x)^2 \\
& -2\varepsilon^{3(\lambda)}\varepsilon^{*3(\lambda)}\sqrt{NN'}2eBI_{N'-1, N-1}(x)I_{N', N}(x) \\
& +\varepsilon_+\varepsilon_+^*(E'_0 \mp m)(E'_0 - \omega \pm m)I_{N'-1, N}(x)^2 \\
& -\sqrt{2N'eB}\omega \cos \theta I_{N'-1, N}(x)I_{N', N}(x)[\varepsilon_+\varepsilon^{*3(\lambda)}e^{-i\varphi} + \varepsilon^{3(\lambda)}\varepsilon_+^*e^{i\varphi}] \\
& +\varepsilon^{3(\lambda)}\varepsilon^{*3(\lambda)}(E'_0 \pm m)(E'_0 - \omega \mp m)I_{N', N}(x)^2.
\end{aligned} \tag{16}$$

Summing over the polarization of the radiation, we have the total unpolarized transition rate

$$\begin{aligned}
\Gamma_{\mp, p'_z=0, \sum \lambda} &= \frac{\alpha}{2} \int_0^{\frac{\pi}{2}} \frac{d\theta \omega \sin \theta}{E'_0[E'_0{}^2 - 2eB(N' - N) \sin^2 \theta]^{1/2}} \{[(E'_0 \mp m)(E'_0 - \omega \pm m)I_{N'-1, N-1}(x)^2 \\
& + (E'_0 \pm m)(E'_0 - \omega \mp m)I_{N', N}(x)^2] \sin^2 \theta + [(E'_0 \pm m)(E'_0 - \omega \mp m)I_{N', N-1}(x)^2 \\
& + (E'_0 \mp m)(E'_0 - \omega \pm m)I_{N'-1, N}(x)^2][1 + (\cos \theta)^2] + 2(\sqrt{2N'eB})\omega[I_{N', N-1}(x) \\
& I_{N'-1, N-1}(x) + I_{N'-1, N}(x)I_{N', N}(x)] \sin \theta (\cos \theta)^2 - 4eB\sqrt{NN'} \\
& \{I_{N', N-1}(x)I_{N'-1, N}(x) + I_{N'-1, N-1}(x)I_{N', N}(x)\}(\sin \theta)^2\}.
\end{aligned} \tag{17}$$

As noted by Herold et al. (1982), the most important transition for astrophysical applications is the transition from $N' = 1$ to $N = 0$. For this case, the rate becomes

$$\begin{aligned}
\Gamma_{(\mp, p'_z=0)} &= \frac{\alpha}{2} \int_0^{\frac{\pi}{2}} \frac{\omega \sin \theta d\theta}{E'_0(E'_0 - \omega \sin^2 \theta)} e^{-\left(\frac{\omega^2 \sin^2 \theta}{2m^2 B'}\right)} \\
& [\varepsilon_+\varepsilon_+^*(E'_0 \mp m)(E'_0 - \omega \pm m) - \omega^2 \sin \theta \cos \theta (\varepsilon_+\varepsilon^{*3(\lambda)}e^{-i\varphi} \\
& + \varepsilon^{3(\lambda)}\varepsilon_+^*e^{i\varphi}) + \varepsilon^{3(\lambda)}\varepsilon^{*3(\lambda)}(E'_0 \pm m)(E'_0 - \omega \mp m)\left(\frac{\omega^2 \sin^2 \theta}{2m^2 B'}\right)].
\end{aligned} \tag{18}$$

Explicitly, for the transition from $N' = 1$ to $N = 0$, one has for polarization $\lambda = 1$

$$\begin{aligned}
\Gamma_{(\mp, p'_z=0)}^{1 \rightarrow 0} &= \frac{\alpha}{2} \int_0^{\frac{\pi}{2}} \frac{\omega \sin \theta d\theta}{E'_0(E'_0 - \omega \sin^2 \theta)} e^{-\left(\frac{\omega^2 \sin^2 \theta}{2m^2 B'}\right)} [(E'_0 \pm m)(E'_0 - \omega \mp m)\frac{\omega^2 \sin^4 \theta}{2m^2 B'} \\
& + (E'_0 \mp m)(E'_0 - \omega \pm m) \cos^2 \theta + 2\omega^2 \sin^2 \theta \cos^2 \theta];
\end{aligned} \tag{19}$$

and for polarization $\lambda = 2$

$$\Gamma_{(\mp, p'_z=0)}^{1 \rightarrow 0} = \frac{\alpha}{2} \int_0^{\frac{\pi}{2}} \frac{\omega \sin \theta d\theta}{E'_0(E'_0 - \omega \sin^2 \theta)} e^{-\left(\frac{\omega^2 \sin^2 \theta}{2m^2 B'}\right)} [(E'_0 \mp m)(E'_0 - \omega \pm m)]. \tag{20}$$

From the above expressions, we calculate the transition rate for unpolarized radiation and obtain the same result as the expression for unpolarized radiation previously calculated by Herold & Ruder (1982).

Now, taking the non-relativistic case, and for transition $N' = 1$ to $N = 0$, we then get that $E'_0 \approx m + mB'$, $\omega \approx mB'$ and the argument of the Laguerre function is $[\frac{\omega^2}{2eB}] \approx \frac{B' \sin^2 \theta}{2}$. Then we confirm the results in Herold et al. (1982) for the non-relativistic transition rates which was given for the case of: $N' = 1$ to 0; $p'_z = 0$ and sum over final electron spins and photon polarizations.

Consider the spin-averaged total cyclotron transition rate for the transition to the fundamental state ($N' \rightarrow N = 0$) and $p'_z = 0$

$$\bar{\Gamma} = \frac{2B'N'^{N'}}{\tau_0(N' - 1)!(1 + 2B'N')^{3/2}} \cdot \int_0^1 dy e^{\frac{-N'(1-\rho)}{(1+\rho)}} \cdot \frac{(1 - \rho)^{N'-1}}{(1 + \rho)^{N'+1}}.$$

$$\begin{cases} 2B'N' - \frac{(1-\rho)}{\rho}; & (\text{sum over } \lambda, \text{ see eq. (27b), Latal 1986}) \\ B'N'; & (\lambda = 2) \\ B'N' - \frac{(1-\rho)}{\rho}; & (\lambda = 1) \end{cases} \quad (21)$$

with $\tau_0 = \frac{1}{\alpha m}$, which is the characteristic time, and $\rho = \sqrt{\frac{(1+2B'N'y^2)}{(1+2B'N')}} with $y = \cos \theta$. By summing over the final state of the electron's spin, the cyclotron transition rate to the ground state is obtained for the spin-up or spin-down initial state,$

$$\Gamma_{\pm}^{N' \rightarrow N=0} = \frac{2B'N'^{N'}}{\tau_0(N'-1)!(1+2B'N')^{3/2}} \cdot \int_0^1 dy e^{-\frac{N'(1-\rho)}{(1+\rho)y}} \cdot \frac{(1-\rho)^{N'-1}}{(1+\rho)^{N'+1}} \cdot \begin{cases} [2B'N' - \frac{(1-\rho)}{\rho}] \cdot [1 \mp \frac{1}{\sqrt{1+2B'N'}}] & (\text{sum over } \lambda) \\ \frac{B'N'}{\rho} \cdot [\rho \mp \frac{1}{\sqrt{1+2B'N'}}]; & (\lambda = 2) \\ \frac{B'N'}{\rho} \cdot [\frac{2y^2}{1+\rho} \cdot [1 \mp \frac{1}{\sqrt{1+2B'N'}}] + \frac{1-\rho}{1+\rho} [\rho \pm \frac{1}{\sqrt{1+2B'N'}}]] & (\lambda = 1). \end{cases} \quad (22)$$

Here the upper sign is for the spin-up case and the lower sign is for the spin-down case.

4 APPROXIMATIONS

We obtain transition rates for any polarization of radiation in the non-relativistic approximation case. For initial electron spin down and transition $N' = 1$ to $N = 0$

$$\Gamma_{(-)}^{1 \rightarrow 0} = \frac{1}{3} \alpha m (B')^2 \quad \text{for } \lambda = 1, \quad (23)$$

$$\Gamma_{(-)}^{1 \rightarrow 0} = \alpha m (B')^2 \quad \text{for } \lambda = 2. \quad (24)$$

For initial electron spin up, one has

$$\Gamma_{(+)}^{1 \rightarrow 0} = \frac{1}{2} \alpha m (B')^3 \quad \text{for } \lambda = 1, \quad (25)$$

$$\Gamma_{(+)}^{1 \rightarrow 0} = \frac{1}{6} \alpha m (B')^3 \quad \text{for } \lambda = 2. \quad (26)$$

Thus the transition rate for linear polarization $\hat{\epsilon}^{(1)}$ is three times smaller (larger) than for $\hat{\epsilon}^{(2)}$ if the initial electron spin is down (up).

For the transition from $N' \rightarrow N = N' - 1$ the rates are

$$\Gamma_{(-)}^{N' \rightarrow N=N'-1} = \frac{1}{3} \alpha m (B')^2 N' \quad \text{for } \lambda = 1, \quad (27)$$

$$\Gamma_{(-)}^{N' \rightarrow N=N'-1} = \alpha m (B')^2 N' \quad \text{for } \lambda = 2, \quad (28)$$

and for $N' \rightarrow N = 0$ the rates are

$$\Gamma_{(+)}^{N' \rightarrow N=0} = \frac{\alpha m B'^{(N'+2)} N'^{(2N'+1)} 2^{(N'-1)} (N')!}{(2N')!} \quad \text{for } \lambda = 1, \quad (29)$$

$$\Gamma_{(+)}^{N' \rightarrow N=0} = \frac{\alpha m B'^{(N'+2)} N'^{(2N'+1)} 2^{(N'-1)} (N')!}{(2N'+1)!} \quad \text{for } \lambda = 2. \quad (30)$$

For the case of circular polarization, we obtain for $p'_z = 0$,

$$\Gamma_{(-)}^{N' \rightarrow N'-1} = \alpha m (B')^2 N' \begin{cases} \frac{1}{6} & \text{for } \lambda = +, \\ \frac{7}{6} & \text{for } \lambda = -. \end{cases} \quad (31)$$

For transitions from N' to N , with initial and final electron spin down (no spin flip) we have

$$\Gamma_{(-)}^{N' \rightarrow N} = \frac{\alpha(B')^{N'-N+1}(N'-N)^{2N'-2N-1} \cdot m(N')!}{[(N'-N-1)!]^2(N)!} \cdot 2^{(N-N')} \cdot \left[\frac{(N'-N-1)! \cdot 2^{2N'-2N}(N'-N+1)!}{[2(N'-N)+1]!} \mp \frac{1}{(N'-N)} \right], \quad (32)$$

where the upper sign is for the polarization $\lambda = +$ and the lower sign is for the polarization $\lambda = -$. By summing over electron initial and final spin states, we obtain

$$\Gamma_{(N>0)}^{N' \rightarrow N} = \frac{\alpha m B'^{N'-N+1} (N'-N+1)(N'-N)^{2N'-2N} 2^{N'-N+1} (N'+N)(N'-1)!}{(2N'-2N+1)!N!} \text{ sum over } \lambda \quad (33)$$

$$\Gamma_{(N>0)}^{N' \rightarrow N} = \frac{\alpha m B'^{(N'-N+1)} (N'-N)^{(2N'-2N)} 2^{(N'-N)} (N'+N)(N'-1)!}{(2N'-2N+1)!N!} \quad \text{for } \lambda = 1, \quad (34)$$

$$\Gamma_{(N>0)}^{N' \rightarrow N} = \frac{\alpha m B'^{(N'-N+1)} (N'-N)^{(2N'-2N)} 2^{(N'-N)} (N'+N)(N'-1)!}{(2N'-2N)!N!} \quad \text{for } \lambda = 2. \quad (35)$$

For the case of circular polarizations (the upper sign means $\lambda = +$ and the lower sign means $\lambda = -$)

$$\Gamma_{(N>0)}^{N' \rightarrow N} = \frac{\alpha(B')^{N'-N+1}(N'-N)^{2N'-2N-1} \cdot m \cdot (N'-1)!((N'+N))}{[(N'-N-1)!(N)!]} \cdot 2^{(N-N'+1)} \cdot \left[\frac{(N'-N+1) \cdot 2^{2N'-2N-1}(N'-N)!}{[2(N'-N)+1]!} \mp \frac{1}{2(N'-N)!} \right]. \quad (36)$$

For the case that the electron spin is \uparrow, \uparrow , with $N > 0$, we obtain

$$\Gamma_{\uparrow, \uparrow}^{N' \rightarrow N} = \frac{\alpha m 2^{N'-N} (B')^{N'-N+1} (N'-1)! (N'-N)^{2N'-2N}}{[2(N'-N)+1]!(N!)} \quad \text{for } \lambda = 1, \quad (37)$$

$$\Gamma_{\uparrow, \uparrow}^{N' \rightarrow N} = \frac{\alpha m 2^{N'-N} (B')^{N'-N+1} (N'-1)! (N'-N)^{2N'-2N}}{[2(N'-N)]!(N!)} \quad \text{for } \lambda = 2, \quad (38)$$

$$\Gamma_{\uparrow, \uparrow}^{N' \rightarrow N} = \frac{\alpha m 2^{N'-N+1} (B')^{N'-N+1} (N'-1)! (N'-N)^{2N'-2N} \cdot (N'-N+1)}{[2(N'-N)+1]!(N!)} \text{ sum over } \lambda. \quad (39)$$

For circular polarizations, we find

$$\Gamma_{\uparrow, \uparrow}^{N' \rightarrow N} = \frac{\alpha m 2^{N-N'} (B')^{N'-N+1} (N'-1)! (N'-N)^{2N'-2N-1}}{[N'-N-1]!^2(N!)} \cdot \left[\frac{2^{2(N'-N)} \cdot (N'-N-1)! (N'-N+1)!}{[2(N'-N)+1]!} \mp \frac{1}{(N'-N)} \right] \quad (40)$$

(with upper sign for $\lambda = +$ and lower sign for $\lambda = -$). For $N = N' - 1$, we obtain

$$\Gamma_{\uparrow, \uparrow, N>0}^{N' \rightarrow N'-1} = m \alpha (B')^2 \cdot \begin{cases} \frac{1}{3} & \text{if } \lambda = 1, \\ 1 & \text{if } \lambda = 2, \\ \frac{1}{6} & \text{if } \lambda = +, \\ \frac{7}{6} & \text{if } \lambda = -, \\ \frac{4}{3} & \text{sum over } \lambda. \end{cases} \quad (41)$$

For electron spin \uparrow, \downarrow we obtain

$$\Gamma_{\uparrow, \downarrow}^{N' \rightarrow N} = \frac{\alpha m 2^{N'-N} (B')^{N'-N+2} (N'-1)! (N'-N)^{2N'-2N+3} (N'-N+1)!}{[(N'-N)!]^2 (N!) [2(N'-N+1)]!} \cdot \begin{cases} \frac{1}{2(N'-N+1)+1} \cdot [4(N'-N+1)! + 4(N'-N)! + 3(N'-N-1)!] & \text{for } \lambda = 1 \\ (N'-N-1)! & \text{for } \lambda = 2 \\ \{(N'-N-1)! + \frac{1}{[2(N'-N+1)+1]} \cdot [4(N'-N+1)! + 4(N'-N)! + 3(N'-N-1)!]\} & \text{sum over } \lambda \end{cases} \quad (42)$$

and for circular polarization we get

$$\begin{aligned} \Gamma_{\uparrow, \downarrow}^{N' \rightarrow N} &= \frac{\alpha m 2^{N'-N} (B')^{N'-N+2} (N'-1)! (N'-N)^{2N'-2N+3}}{[(N'-N)!]^2 (N!) [2(N'-N+1)]!} \cdot [2(2N'-2N+1) \frac{[(N'-N+1)]^2}{(2(N'-N+1)+1)!} \\ &\mp \frac{(N'-N)!}{2(N'-N+1)!} + 2^{2N'-2N+1} \frac{(N'-N)! (N'-N+1)!}{[2(N'-N+1)+1]!} + 2^{2N'-2N-1} \frac{(N'-N-1)! (N'-N+1)!}{[2(N'-N+1)]!} \\ &\mp \frac{(N'-N-1)!}{2(N'-N+1)!} + \frac{3 \cdot 2^{2N'-2N-1} (N'-N-1)! (N'-N+1)!}{[2(N'-N+1)+1]!}], \end{aligned} \quad (43)$$

where the upper sign is for $\lambda = +$, and the lower sign is for $\lambda = -$. For the transition $N' \rightarrow N' - 1$ the non-relativistic approximations are

$$\Gamma_{\uparrow, \downarrow}^{N' \rightarrow N'-1} = \begin{cases} \frac{1}{2} \alpha m (B')^3 & \text{for } \lambda = 1, \\ \frac{1}{6} \alpha m (B')^3 & \text{for } \lambda = 2, \\ \frac{2}{3} \alpha m (B')^3 & \text{sum over } \lambda, \\ \frac{1}{12} \alpha m (B')^3 & \text{for } \lambda = +, \\ \frac{7}{12} \alpha m (B')^3 & \text{for } \lambda = -. \end{cases} \quad (44)$$

5 RESULTS

5.1 Sample Calculated Transition Rates

We now return to calculating the full relativistic transition rates. For the transitions $N' = 1$ to $N = 0$, $p'_z = 0$, and the range of magnetic field strengths $0.1 \leq B' \leq 20$, which is supposed to exist in magnetars, cyclotron rates are shown in Figure 1. The transition rate is greatest for polarization $\hat{\epsilon}^{(2)}$ (perpendicular) and electron spin down-down ($\downarrow\downarrow$). Also, for B' greater than 2.36, the rate for $\hat{\epsilon}^{(1)}$ (parallel) polarization and electron spin $\uparrow\downarrow$ becomes larger than the rate for $\hat{\epsilon}^{(1)}$ (parallel) polarization and electron spin $\downarrow\downarrow$.

For the $N' = 2$ to $N = 1$ case and spin orientation $\downarrow\downarrow$, one also finds that the rate for polarization $\hat{\epsilon}^{(2)}$ is larger than for $\hat{\epsilon}^{(1)}$, as is also true for the $N' = 1$ to $N = 0$ case. Figure 2 shows the transition rate in units of the cyclotron frequency ω_B . The effect of nonzero p'_z is also shown in Figure 2: increasing p'_z decreases the transition rate.

In Figure 3, we compare transition rates for different Landau level transitions with the initial level $N' = 3$ (taking $p'_z = 0$). Transition rates for polarization $\hat{\epsilon}^{(2)}$ are generally larger than rates for polarization $\hat{\epsilon}^{(1)}$. For polarization $\hat{\epsilon}^{(2)}$, when $B < \sim 1.4B_{\text{cr}}$, the highest rate is for the Landau transition $N' = 3$ to $N = 2$ but when $B > 1.4B_{\text{cr}}$, the highest rate is for the Landau transition $N' = 3$ to $N = 0$. For polarization $\hat{\epsilon}^{(1)}$, when $B < \sim 8B_{\text{cr}}$, the highest rate is for the Landau transition $N' = 3$ to $N = 2$, but when $B > 8B_{\text{cr}}$, the highest rate is for the Landau transition $N' = 3$ to $N = 0$.

The transition rates for different types of photon polarization and for transitions from $N' = 20$ to all different $N < N'$ are shown in Figure 4. These were calculated for the case $B = 1B_{\text{cr}}$, $p'_z = 0$ and for electron spin $\downarrow\downarrow$. One always finds the result $\Gamma_{\hat{\epsilon}^{(2)}} > \Gamma_{\hat{\epsilon}^{(+)}} = \Gamma_{\hat{\epsilon}^{(-)}} > \Gamma_{\hat{\epsilon}^{(1)}}$.

Next, we consider a non-relativistic thermal electron energy distribution

$$f^{\text{th}}(p_z) = \frac{1}{2(2\pi mT)^{1/2}} e^{(-\frac{p_z^2}{2mT})}, \quad (45)$$

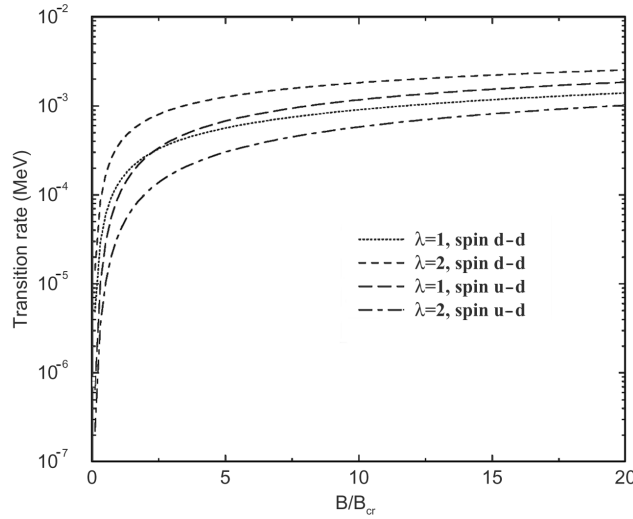


Fig. 1 Transition rates for different types of photon polarizations and for transitions from $N' = 20$ to $N < N'$.

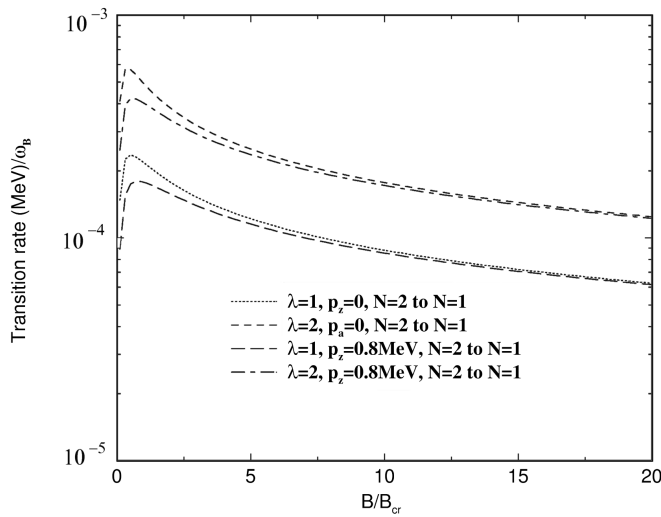


Fig. 2 Transition rate (divided by ω_B) vs. magnetic field for $N' = 2$ to $N = 1$ and spin orientation $\downarrow\downarrow$.

and obtain emission rates vs. frequency (i.e. spectra) for linearly polarized photons. We consider the case for temperature $T = 0.02m \approx 10$ keV and $\theta = 30^\circ$.

Figure 5 shows the results for the transition $N' = 1$ to $N = 0$ and $\frac{B}{B_{cr}} = 0.1$. The result for the sum over photon polarizations is similar to Herold et al. (1982). The photon emission rate is larger for electron initial spin down than for spin up.

Also, we see for $B = 0.1B_{cr}$ that the emission rate is larger by a factor of ~ 20 for photon polarization $\varepsilon^{(\lambda=2)}$ than for $\varepsilon^{(\lambda=1)}$. In Figure 6, we show the results for $B = 10B_{cr}$ and summing

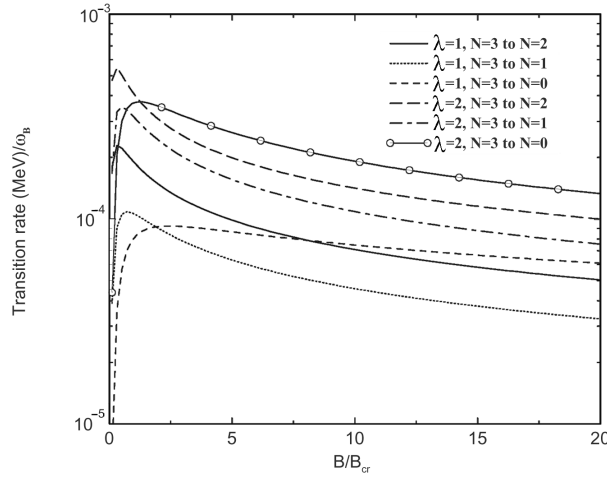


Fig. 3 Transition rates (divided by ω_B) from the $N = 3$ Landau level, with $p_z = 0$.

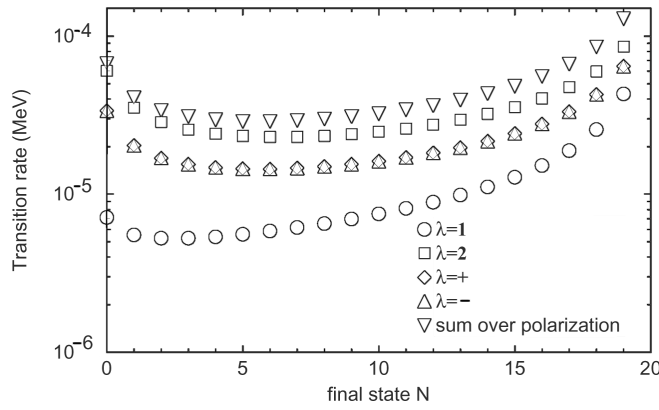


Fig. 4 Transition rates for different types of photon polarization and for transitions from $N' = 20$ to $N < N'$.

over Landau transitions N' to $N = 0$ for $N' = 1$ to 10. The radiation spectrum resulting from each transition is much narrower and is at a lower frequency relative to the cyclotron frequency than for smaller B . Thus, one can see the separate emissions from the different Landau transitions in the spectrum, and hence there are 10 peaks in the spectrum, limited by the number of Landau transitions we chose to calculate.

Lastly, we consider the emission spectra from non-thermal electrons, using the distribution function of Herold et al. (1982)

$$f^{nt}(p_z) = \frac{1}{2\pi(2mT)^{1/2}} \left(1 + \frac{p_z^2}{2mT}\right)^{-1}. \tag{46}$$

We calculate emission rates vs. frequency for unpolarized and linearly polarized photons and we sum over all Landau transitions N' to $N = 0$ for $N' = 1$ to 10.

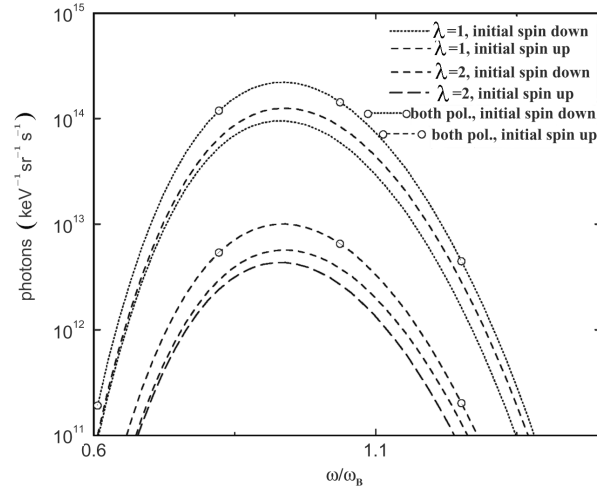


Fig. 5 Photon emission rate vs. frequency in units of cyclotron frequency, ω_B , for a thermal electron energy distribution with temperature 10 keV. Rates are shown for the different photon polarizations and initial electron spins and for $B = 0.1B_{\text{cr}}$.

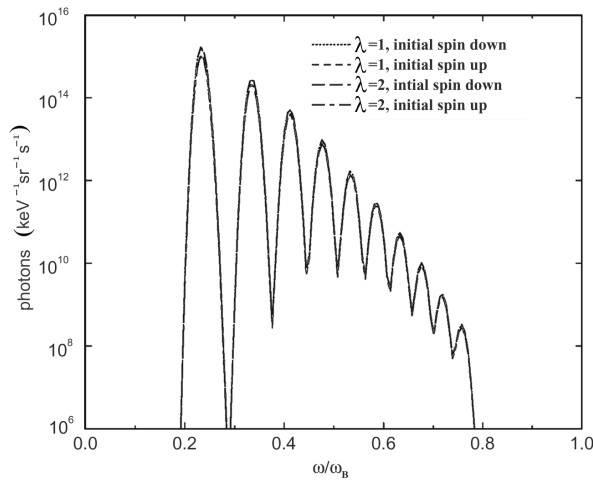


Fig. 6 Results for $B = 10 B_{\text{cr}}$.

We take $T = 0.02m \approx 10 \text{ keV}$ and $\theta = 5^\circ$. Figure 7 shows the results for the $B = 0.1B_{\text{cr}}$ and $B = B_{\text{cr}}$.

Figure 8 shows the results for the $B = B_{\text{cr}}$ and $B = 10B_{\text{cr}}$. As B increases, the spectrum becomes narrower and, although it shifts to a higher energy relative to the cyclotron frequency, the spectrum shifts lower. The photon emission rate is larger for electron initial spin down than for spin up, although the difference is quite small (only visible at the highest frequencies on these plots). Also, we see that the emission rate is larger for photon polarization $\varepsilon^{(\lambda=2)}$ than for $\varepsilon^{(\lambda=1)}$ by factors ~ 20 , ~ 5 , and ~ 1.6 for $B = 0.1$, 1, and $10 B_{\text{cr}}$, respectively.

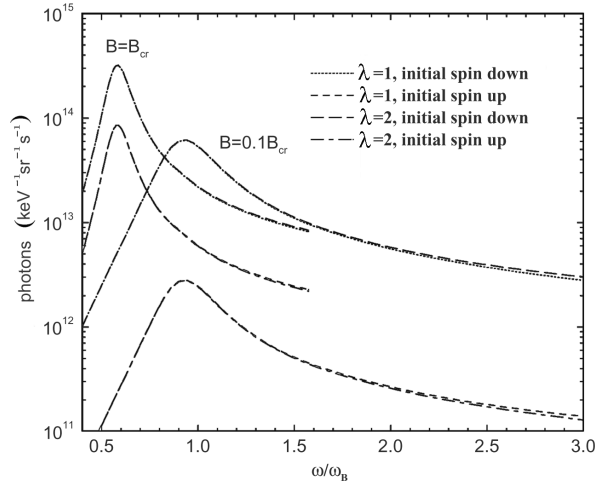


Fig. 7 Photon emission rate vs. frequency, in units of the cyclotron frequency, ω_B , for the non-thermal electron energy distribution of Herold et al. (1982) with $T = 10$ keV. Rates are shown for the different photon polarizations and initial electron spins. Results are for the cases $B = 0.1B_{cr}$ and $B = B_{cr}$.

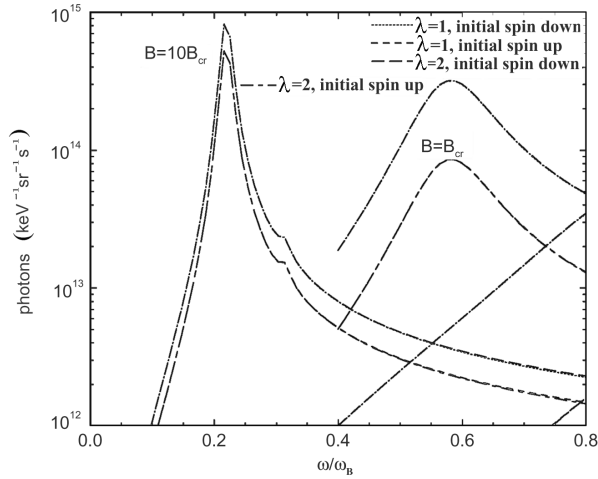


Fig. 8 Results for $B = B_{cr}$ and $B = 10B_{cr}$.

If we now analyze the spin-dependent absorption cross section in the frame of a non-relativistic limit, for both linear polarizations, and by using equation (2) of Harding & Daugherty (1991), we obtain the following expression (the electron spins are initially in the ground state)

$$\sigma_{abs}^{N,1}(\theta) \sim \frac{\alpha\pi^2\hbar^2c^2}{m} \cdot \frac{B'N}{(N-1)!} \cdot \left(\frac{N^2B'\sin^2\theta}{2}\right)^{N-1}. \quad (47)$$

This is valid for the case of $\lambda = 1$ and for spin $\downarrow\uparrow$ (spin down-up) and

$$\sigma_{\text{abs}}^{N,1}(\theta) \sim \frac{\alpha\pi^2\hbar^2c^2}{m} \cdot \frac{B'N}{(N-1)!} \cdot \left(\frac{N^2B'\sin^2\theta}{2}\right)^{N-1} \cdot \cos^2\theta, \quad (48)$$

again valid for the case with $\lambda = 2$ and for spin $\downarrow\uparrow$ (spin down-up).

Additionally, for the cases of spin ($\downarrow\downarrow$) down-down we got

$$\sigma_{\text{abs}}^{N,2}(\theta) \sim \frac{\alpha\pi^2\hbar^2c^2}{m} \cdot \frac{1}{(N-1)!} \cdot \left(\frac{N^2B'\sin^2\theta}{2}\right)^{N-1} \cdot (2\cos^2\theta)(1 - NB'\sin^2\theta), \quad (49)$$

for $\lambda = 1$, and

$$\sigma_{\text{abs}}^{N,2}(\theta) \sim \frac{2\alpha\pi^2\hbar^2c^2}{m} \cdot \frac{1}{(N-1)!} \cdot \left(\frac{N^2B'\sin^2\theta}{2}\right)^{N-1}, \quad (50)$$

for $\lambda = 2$.

Thus, if we now average over the photon polarizations described by Equations (48), (49), (50) and (51), we just obtain equation (14) (Harding & Daugherty 1991), except that we get a factor of two difference for the second equation (14) of their paper cited above, and we get

$$\sigma_{\text{abs}}^{N,2}(\theta) \sim \frac{\alpha\pi^2\hbar^2c^2}{m} \cdot \frac{1}{(N-1)!} \cdot \left(\frac{N^2B'\sin^2\theta}{2}\right)^{N-1} \cdot [(1 + \cos^2\theta) - NB'\sin^2\theta\cos^2\theta]. \quad (51)$$

Thus, the evaluation of the total absorption cross section, including the spin-dependent natural line width for the first harmonic ($N = 1$), for the linear polarization, yields

$$\sigma_{\text{abs}}^1 = \sigma_{\text{abs}}^{1,1} \frac{2}{\pi\Gamma_{1,1}} + \sigma_{\text{abs}}^{1,2} \frac{2}{\pi\Gamma_{1,2}} \sim \frac{4\pi\hbar^2c^2}{m^2B'^2} \cdot (1 + 3\cos^2\theta) \quad (52)$$

(for either $\lambda = 1$ or $\lambda = 2$).

Figure 9 shows the total absorption cross section, including natural line width for the first five harmonics, when initially the electrons are in the ground state, $B = 0.1$ and $\theta = 30^\circ$. Applying equation (9) used by Harding & Daugherty (1991), and for the case of linear polarization and unpolarized absorbed radiation. Equations (47), (48), (49) and (50) were used and transition rates in non-relativistic approximation for emission processes. Also by summing over the orientation of the electron is in the final state, because initially if $N = 0$, only the spin-down orientation is permitted.

Figure 10 displays the total transition rate for magnetic strength beyond the critical field. The non relativistic approximation behaves as a straight line, growing linearly whereas the exact total transition declines after a value greater than the critical field according to Herold et al. (1982).

5.2 Application to Neutron Stars

The detection of cyclotron lines in neutron stars allows a direct determination of the magnetic field intensity. In the case of the pulsar Her X-1, Truemper et al. (1978) suggested the existence of a strong line feature at ~ 58 keV in the pulsed (1.24 s) X-ray spectrum and the interpretation of this line is a consequence of the electron cyclotron emission. This feature is now generally accepted as an absorption line around 40 keV (see, R. Staubert et al. 2007).

For the evaluation of the magnetic field strength, we also take the gravitational redshift into account. For the non-relativistic case, with $p'_z = 0$ and $\theta = \frac{\pi}{2}$, the fundamental line (transition from $N' = 1 \rightarrow 0$) has $E_0 \sim mB'(1 + Z_g)^{-1}(\text{MeV}) = 11.6 \frac{B}{10^{12}\text{G}}(1 + Z_g)^{-1}(\text{keV})$ and the other harmonic lines, i.e., $2E_0, 3E_0, \dots$, are given by expression of equation (1) in Coburn et al. (2002). However, it should be emphasized that this is only valid for very strong magnetic fields

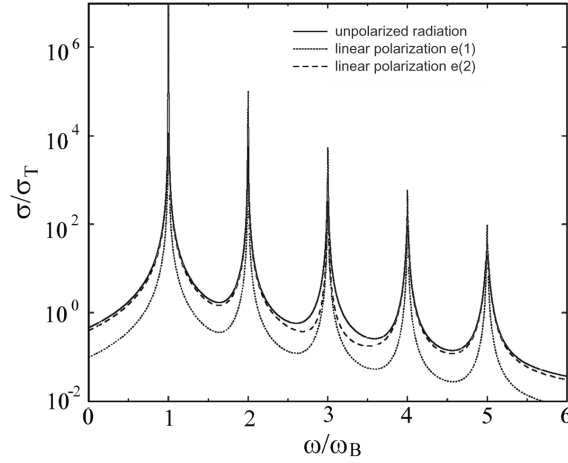


Fig. 9 Absorption cross sections with spin-dependent relativistic natural width as a function of incident energy (in units of the cyclotron energy) and for unpolarized absorbed radiation for both linear polarizations, for field strength $B' = 0.1$ and photon angle $= 30^\circ$. We used the nonrelativistic approximation expressions for this figure and obtained similar results as fig. 1 of the paper (Harding & Daugherty 1991).

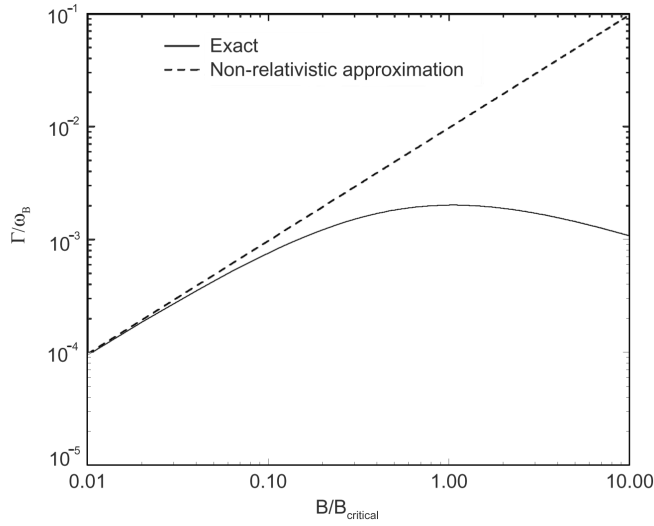


Fig. 10 Total transition rates in units of ω_B , so that we can compare with fig. 2 of Herold et al. (1982). In that paper they analyze the same process, but by summing over polarizations of the radiation. We obtain the same result for unpolarized radiation if the spin orientation is down-down. For a fairly weak magnetic field, both solutions, non-relativistic and relativistic, give the same solutions. However, for B near B_{cr} , we have a different value for each solution. Specifically, we analyze the transition from $N = 1$ to $N = 0$ and $p_z = 0$ MeV.

$B' \sim 1$. Thus, we must use the exact expression for the transition rates because the difference in the percentage for the transitions is quite large, i.e. $N = 1 \rightarrow 0$: 38% difference; $N = 2 \rightarrow 0$: 60% difference; and $N = 3 \rightarrow 0$: 80% difference. For the case of Her X-1, the gravitational redshift, $Z_g = 0.305$, can be calculated by using Leahy (2004): $M = 1.4M_\odot$ and $R = 10^6$ cm. Thus, the observed energy is given by $E_{0,\text{obs}} = E_0(1 + Z_g)^{-1}$. Heindl et al. (2004) suggested a magnetic field strength of $B = 3.5 \times 10^{12}$ G to obtain the observed absorption line at ~ 41 keV. However, as we have noted, the errors in using the approximate expression for ω are significant. We find we need to take $B = 5.0 \times 10^{12}$ G in order to obtain the fundamental at the energy of 41 keV. As discussed above, the emitted radiation is dominated by linear polarization $\hat{\varepsilon}^{(2)}$.

V0332+53 has several observed cyclotron resonance features (CRSFs). Pottschmidt et al. (2005) confirm the presence of three absorption line energies: the fundamental line has $\omega = 26.3$ keV, the second cyclotron line energy is ~ 50 keV and the third line energy is 73.7 keV. We evaluate line energies corrected for redshift using our formulae for different values of the magnetic field. In Table 3, we present a set of energies matching those observed for V0332+53; to match the observed lines of V0332+53, we find that the required strength of the magnetic field is $\simeq 3.1 \times 10^{12}$ G. In Table 3, the values enclosed by parentheses are the average values of the cyclotron energy emitted near the surface of the neutron star. The values before the parentheses are the average energy values far from the star when we take into account gravitational redshift.

Table 3 Energy of the First Five Transitions to the Ground State for V0332+53, for $B = 3.1 \times 10^{12}$ G

Transitions	$\bar{\omega}$ (keV) for $\hat{\varepsilon}^{(1)}$	$\bar{\omega}$ (keV) for $\hat{\varepsilon}^{(2)}$	Probability for $\hat{\varepsilon}^{(1)}$ (%)	Probability for $\hat{\varepsilon}^{(2)}$ (%)
1 \rightarrow 0	26.1 (34)	26.3 (34)	25.2	74.8
2 \rightarrow 0	50.3 (66)	51 (67)	17.1	82.9
3 \rightarrow 0	73 (95)	74.3 (97)	13.1	86.9
4 \rightarrow 0	95 (124)	96.6 (126)	10.8	89.2
5 \rightarrow 0	115.8 (151)	117.9 (154)	9.2	90.8

6 SUMMARY

In this paper, we have presented new calculations which extend previous works. We present complete formulae to calculate fully relativistic cyclotron transition rates for an arbitrary magnetic field, for any orientation of electron's spin and for any polarization of emitted radiation. Also, we obtain the transition rates for any value of the initial electron's parallel momentum. The formulae have been applied to calculate cyclotron emission rates for a number of sample cases, with different magnetic fields, different polarizations and electron spins, different Landau transitions and different electron momenta or electron momentum distributions. These formulae should be useful in calculating cyclotron emission rates for cases of strong magnetic fields, such as for accreting neutron stars and magnetars, and to obtain the rates for the different photon polarizations and electron spin states of interest.

Acknowledgements L.S. acknowledges support from MICIT (Ministry of Science and Technology) and CONICIT of Costa Rica. We acknowledge support from the Natural Sciences and Engineering Research Council of Canada.

Appendix A:

We carry out our calculations in the Landau gauge and use electron wave functions of Herold (1979), and Sokolov & Ternov (1968)

$$\Psi^1(\mathbf{r}, t) = (eB)^{1/4} \frac{e^{i(p_y y + p_z z - Et)}}{(L_z L_y)^{1/2} 2[EE_0(E + E_0)]^{1/2}} \times \begin{pmatrix} -ip_z(E_0 - m)^{1/2} \Phi_{N-1}(\rho) \\ (E + E_0)(E_0 + m)^{1/2} \Phi_N(\rho) \\ -i(E + E_0)(E_0 - m)^{1/2} \Phi_{N-1}(\rho) \\ -p_z(E_0 + m)^{1/2} \Phi_N(\rho) \end{pmatrix} \quad (\text{A.1})$$

which corresponds to spin down, and

$$\Psi^2(\mathbf{r}, t) = (eB)^{1/4} \frac{e^{i(p_y y + p_z z - Et)}}{(L_z L_y)^{1/2} 2[EE_0(E + E_0)]^{1/2}} \times \begin{pmatrix} (E + E_0)(E_0 + m)^{1/2} \Phi_{N-1}(\rho) \\ -ip_z(E_0 - m)^{1/2} \Phi_N(\rho) \\ p_z(E_0 + m)^{1/2} \Phi_{N-1}(\rho) \\ i(E + E_0)(E_0 - m)^{1/2} \Phi_N(\rho) \end{pmatrix} \quad (\text{A.2})$$

which corresponds to spin up. In the above: $E_0 = \sqrt{m^2 + 2NeB} = m\sqrt{1 + 2NB'}$, and $\Phi_N(\rho)$ are the normalized eigenfunctions of the one-dimensional harmonic oscillator with the argument $\rho = \sqrt{eB}(x + \frac{p_y}{eB})$: $\Phi_N(\rho) = (\frac{eB}{\pi})^{1/4} (2^N N!)^{-1/2} H_N(\rho) e^{-\frac{\rho^2}{2}}$. The polarization of the photon is denoted by $\lambda = 1, 2$ (linear polarization) or $+, -$ (circular polarization). $\hat{\varepsilon}^{(1)}$ (also denoted $||$) and $\hat{\varepsilon}^{(2)}$ (also denoted \perp), have the photon's electric field respectively parallel or orthogonal to $\mathbf{k} \times \mathbf{B}$. The unit vectors $\hat{\varepsilon}^{(1)}$, $\hat{\varepsilon}^{(2)}$, and \hat{k} form a right-handed coordinate system:

$$\hat{\varepsilon}^{(1)} \times \hat{\varepsilon}^{(2)} = \hat{k}. \quad (\text{A.3})$$

The integrals for the transition rates are

$$\begin{aligned} I_1 &= \int_{-\infty}^{\infty} e^{-ik_x x} \Phi_{N-1}(\rho) \Phi_{N'}(\rho) dx \\ &= e^{\frac{+ik_x p_y}{eB}} (-i)^{N'-N+1} e^{i\varphi(N'-N+1)} e^{\frac{i\omega^2 \sin^2 \theta \sin 2\varphi}{4eB}} \cdot I_{N', N-1} \left(\frac{\omega_{\perp}^2}{2eB} \right) \end{aligned} \quad (\text{A.4})$$

for $N' \geq N - 1$, with $\omega_{\perp} = \omega \sin \theta$ and $\rho = \sqrt{eB}(x + \frac{p_y}{eB})$;

$$\begin{aligned} I_2 &= \int_{-\infty}^{\infty} e^{-ik_x x} \Phi_{N-1}(\rho) \Phi_{N'-1}(\rho) dx \\ &= e^{\frac{+ik_x p_y}{eB}} (-i)^{N'-N} e^{i\varphi(N'-N)} e^{\frac{i\omega^2 \sin^2 \theta \sin 2\varphi}{4eB}} \cdot I_{N'-1, N-1} \left(\frac{\omega_{\perp}^2}{2eB} \right) \end{aligned} \quad (\text{A.5})$$

for $N' - 1 \geq N - 1$;

$$\begin{aligned} I_3 &= \int_{-\infty}^{\infty} e^{-ik_x x} \Phi_N(\rho) \Phi_{N'-1}(\rho) dx \\ &= e^{\frac{+ik_x p_y}{eB}} (-i)^{N'-1-N} e^{i\varphi(N'-1-N)} e^{\frac{i\omega^2 \sin^2 \theta \sin 2\varphi}{4eB}} \cdot I_{N'-1, N} \left(\frac{\omega_{\perp}^2}{2eB} \right) \end{aligned} \quad (\text{A.6})$$

for $N' - 1 \geq N$; and

$$\begin{aligned} I_4 &= \int_{-\infty}^{\infty} e^{-ik_x x} \Phi_N(\rho) \Phi_{N'}(\rho) dx \\ &= e^{\frac{+ik_x p_y}{eB}} (-i)^{N'-N} e^{i\varphi(N'-N)} e^{\frac{i\omega^2 \sin^2 \theta \sin 2\varphi}{4eB}} \cdot I_{N', N} \left(\frac{\omega_{\perp}^2}{2eB} \right) \end{aligned} \quad (\text{A.7})$$

for $N' \geq N$. We used Gradshteyn & Ryzhik (1965): Tables of Integrals, Series and Products to evaluate these integrals.

References

- Baring, M. G., Gonthier, P. L., & Harding, A. K. 2005, *ApJ*, 630, 430
- Bezchastnov, V. G., & Pavlov, G. G. 1991, *Ap&SS*, 178, 1
- Coburn, W., Heindl, W. A., Rothschild, R. E., Gruber, D. E., Kreykenbohm, I., Wilms, J., Kretschmar, P., & Staubert, R. 2002, *ApJ*, 580, 394
- Daugherty, J. K., & Ventura, J. 1977, *A&A*, 61, 723
- Daugherty, J. K., & Ventura, J. 1978, *Phys. Rev. D*, 18, 1053
- Gradshteyn, I. S., & Ryzhik, I. M. 1965, *Tables of Integrals Series and Products* (New York: Academic Press)
- Harding, A. K., & Daugherty, J. K. 1991, *ApJ*, 374, 687
- Harding, A. K., & Preece, R. 1987, *ApJ*, 319, 939
- Heindl, W. A., Rothschild, R. E., Coburn, W., Staubert, R., Wilms, J., Kreykenbohm, I., & Kretschmar, P. 2004, *X-ray Timing 2003: Rossi and Beyond*, 714, 323
- Herold, H. 1979, *Phys. Rev. D*, 19, 2868
- Herold, H., Ruder, H., & Wunner, G. 1982, *A&A*, 115, 90
- Herold, H., & Ruder, H. 1982, *Phys. Scr.*, 2, 206
- Latal, H. G. 1986, *ApJ*, 309, 372
- Leahy, D. A. 2004, *ApJ*, 613, 517
- Pavlov, G. G., Bezchastnov, V. G., Meszaros, P., & Alexander, S. G. 1991, *ApJ*, 380, 541
- Pottschmidt, K., et al. 2005, *ApJ*, 634, L97
- Sina, R. 1996, Ph. D. Thesis, August, University of Maryland
- Sokolov, A. A., & Ternov, I. M. 1968, *Synchrotron Radiation* (Berlin: Akademie Verlag)
- Staubert, R., Shakura, N. I., Postnov, K., Wilms, J., Rothschild, R. E., Coburn, W., Rodina, L., & Klochkov, D. 2007, *A&A*, 465, L25
- Truemper, J., Pietsch, W., Reppin, C., Voges, W., Staubert, R., & Kendziorra, E. 1978, *ApJ*, 219, L105